

## A modified variable physical properties model, for analyzing nanofluids flow and heat transfer over nonlinearly stretching sheet

Pooria Akbarzadeh\*

School of Mechanical Engineering, Shahrood University of Technology

Received 16 July 2015;

revised 11 December 2016;

accepted 11 January 2017;

available online 10 June 2017

**ABSTRACT:** In this paper, the problem of laminar nanofluid flow which results from the nonlinear stretching of a flat sheet is investigated numerically. In this paper, a modified variable physical properties model for analyzing nanofluids flow and heat transfer is introduced. In this model, the effective viscosity, density, and thermal conductivity of the solid-liquid mixture (nanofluids) which are commonly utilized in the homogenous single-phase model, are locally combined with the prevalent single-phase model. A numerical similarity solution is considered which depends on the local Prandtl number, local Brownian motion number, local Lewis number, and local thermophoresis number. The results are compared to the prevalent single-phase model. This comparison depicts that the prevalent single-phase model has a considerable deviation for predicting the behavior of nanofluids flow especially in dimensionless temperature and nanoparticle volume fraction. In addition the effect of the governing parameters such as Prandtl number, the Brownian motion number, the thermophoresis parameter, the Lewis number, and etc. on the velocity, temperature, and volume fraction distribution and the dimensionless heat and mass transfer rates are examined.

**KEYWORDS:** *Nanofluid; Nonlinear stretching sheet; Similarity solution; Modified variable physical properties model*

### INTRODUCTION

Improvement in heat transfer characteristics, has an important role in increasing the efficiency of many physical and engineering processes such as cooling of electronic components, bearings heat removal, heat exchangers, cooling of strips or filaments, and to name but a few. One way to enhance the heat transfer characteristics of the original (base) fluid, is the use of nanofluids. Nanofluids are a new class of fluids that contain bases fluid and nanometer-sized particles (such as Cu, Ag, CuO, Al<sub>2</sub>O<sub>3</sub>, TiO<sub>2</sub> and etc. as metallic or metallic oxide particles or MWNTs as metallic nanotubes). One of the possible mechanisms for an outstanding increase in the thermal performance of nanofluids is the Brownian motions of these nanoparticles inside the fluids [1-4]. Till now, there have been published several papers in the field of thermal characteristics of nanofluids flow such as Refs. [1-9] and to name but a few. As mentioned above, one of the application of heat transfer in industries is cooling of continuous strips or filaments by drawing them through a motionless fluid (for example materials manufactured by extrusion, glass-fiber and paper production). In these cases, the final product of desired characteristics depends on the rate of cooling in the process and the process of stretching [10]. In order to predict the heat transfer characteristics of such process, it is required to simulate the boundary layer behaviour of fluid flow over the stretching surface (strips or filaments). After the preliminary works of Sakiadis [11-13] in the subject of

Boundary Layer Flow (BLF) behaviour over a continuous moving surface (with constant velocity), the BLF happened by a stretching surface has stirred up the attention of many researchers. Crane [14] obtained the exact temperature distribution of the steady BLF of a viscous fluid caused by stretching a flat sheet with a linear velocity. He dealt with the isothermal sheet. The heat and mass transfer on a stretching plate with blowing or suction was examined by Gupta and Gupta [15]. They handled the isothermal moving plate and found the temperature and concentration distributions. The same problem was studied by Dutta et al. [16] in which the sheet was subjected to a uniform heat flux without blowing or suction. Chen and Char [17] extended the work of Gupta and Gupta [15] in the case of prescribed stretching sheet temperature and heat flux. The problem of nonlinear stretching sheet for different cases of boundary conditions has also been studied by different researchers. In 2001, Vajravelu [18] examined the boundary layer behavior and thermal characteristics of flow over a nonlinear stretching sheet without considering the viscous dissipation terms. In 2006, Vajravelu and Cannon [19] presented the existence results of the nonlinearly stretching boundary problem. Then Cortell [20] in 2007 studied flow and heat transfer on a nonlinear stretching sheet for two different types of thermal boundary conditions, i.e. prescribed and constant surface temperature. Prasad et al. [21] presented a numerical solution for the steady mixed convection magneto-hydrodynamics flow of an electrically conducting viscous fluid over a stretching sheet with variable fluid properties.

\*Corresponding Author Email: [Akbarzad@ut.ac.ir](mailto:Akbarzad@ut.ac.ir)

Tel.: +989122022776; Note. This manuscript was submitted on July 16, 2015; approved on December 11, 2016; published online June 10, 2017.

Nomenclature	
$a_T, a_u$	positive constants
$D_B$	Brownian diffusion coefficient
$D_T$	thermophoretic diffusion coefficient
$c$	specific heat capacity
$k$	thermal conductivity
$\overline{Le}$	Lewis number
$n, r$	nonlinear stretching parameters
$\overline{Nb}$	Brownian motion number
$\overline{Nt}$	thermophoresis parameter
$Nu$	Nusselt number
$Pr$	Prandtl number
$Re_x$	local Reynolds number
$Sh$	local Sherwood number
$q_m$	surface mass flux
$q_w$	surface heat flux
$T$	temperature of the fluid
$u$	velocity component along $x$
$v$	velocity component along $y$
$x$	coordinate measured along the surface
$y$	coordinate measured normal to the surface
<b>Subscripts</b>	
$f$	base fluid
$nf$	nanofluid
$p$	nanoparticles
$w$	wall surface
$\infty$	far away from the stretching sheet
<b>Greek Symbols</b>	
$\alpha$	thermal diffusivity
$\varphi$	nanoparticle volume fraction
$\rho$	density
$\nu$	kinematic viscosity
$\eta$	similarity parameter
$\theta$	dimensionless temperature
$\psi$	dimensionless nanoparticle volume fraction

Postelnicu and Pop [22] examined the steady two-dimensional laminar BLF of a power-law fluid past a permeable non-linear stretching wedge. Recently, Vajravelu et al. [23] analyzed magneto-hydrodynamics flow and heat transfer of a power-law fluid over an unsteady stretching sheet.

One way to improve the heat transfer characteristics of flow past a stretching sheet, is the use of nanofluids. Bachok et al. [24] studied BLF of nanofluids over a continuous moving surface (with constant velocity). Khan and Pop [25] investigated the temperature distribution of the steady BLF of nanofluids caused by stretching a flat sheet with a linear velocity. They handled the isothermal sheet. Gorder et al. [26] presented the similarity solution for the nano-BLFs over a linearly stretching sheet, in which on the surface sheet, the velocity slip was assumed to be proportional to the local shear stress. Hassani et al. [27] obtained an analytical solution for BLF of a nanofluid past a linearly stretching sheet using homotopy analysis method (HAM). Rana and Bhargava [10] studied numerically the flow and heat transfer of a nanofluid over a nonlinearly stretching sheet. Nadeem et al. [28] analyzed the flow of three-dimensional water-based nanofluid over an exponentially stretching sheet. Das [29] investigated the problem of BLF of a nanofluid over a non-linear permeable stretching sheet at predestined surface temperature in the presence of partial slip.

The numerical works presented in many papers show that, in order to investigate the heat transfer enhancement by nanoparticles (or generally small solid particles) suspended in a fluid, two main approaches have been adopted by researchers. The first approach is the two-phase model, which consider both the fluid and the solid phases role in the heat transfer process. The second one is the single-phase model in which both phases are in thermal and hydrodynamic equilibrium state (this approach is simpler

and more computationally efficient). Generally, in nanofluids, there are several factors that affect heat transfer enhancement. Some of the more important factors are Brownian motion (diffusion, sedimentation, and dispersion), gravity, layering at the solid/liquid interface, particles clustering, the friction between the fluid and the solid particles, and etc. Therefore, in the absence of any experimental data and suitable theoretical studies, the existing macroscopic two-phase model has not enough precision for analyzing nanofluids. Consequently, the modified single-phase, considering some of the above factors, is more convenient than the two-phase model if the main interest of analysis is the heat transfer process [30]. Therefore, in order to improve the results of the single-phase model for analyzing the nanofluids flow, some modifications are needed. In this paper, a new modified single-phase model for analyzing nanofluids flow and heat transfer is introduced for the first time. In this model, all effective properties of nanofluids such as, density, viscosity, and thermal conductivity which are normally used for the effective single-phase model (as constant values), are incorporated locally with the governing equations (as no-constant values). This approach is used for examining the BLF behavior and thermal characteristics of flow over a nonlinear stretching sheet. The results for Cu and  $Al_2O_3$  nanoparticles are compared to the prevalent single-phase model. This comparison depicts that the prevalent single-phase model has a considerable deviation for predicting the behavior of nanofluids flow especially in dimensionless temperature and nanoparticle volume fraction. In addition the effect of the governing parameters such as Prandtl number, the Brownian motion number, the thermophoresis parameter, the Lewis number, and etc. on the velocity, temperature, and volume fraction distribution and the dimensionless heat and mass transfer rates are examined.

**MATHEMATICAL MODEL**

The steady two-dimensional BLF of a nanofluid past a stretching sheet is considered with the nonlinear velocity of  $u_w = a_u x^n$ , where  $a_u$  is a positive constant,  $n$  is nonlinear stretching parameter and  $x$  is the coordinate measured along the stretching surface, as shown in Figure 1. By stretching the sheet, the flow takes place at  $y \geq 0$ , where  $y$  is the coordinate measured normal to the stretching surface. Because of the impermeability characteristic of the sheet, the vertical velocity of fluid on the surface is  $v_w = 0$ . In this problem, the stretching surface is maintained at prescribed surface temperature  $T_w = T_\infty + a_T x^r$ , where  $a_T$  is a positive constant,  $r$  is the surface temperature parameter in the prescribed surface temperature boundary condition and  $T_\infty$  is the temperature of the fluid far away from the stretching sheet. According to Refs. [31] and [32], the following four governing boundary layer equations embody the continuity, momentum, thermal energy, and nanoparticles concentration, respectively:

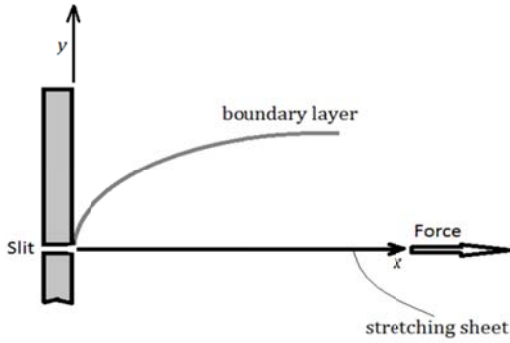


Fig. 1. Physical model of BLF of a nanofluid past a stretching sheet and coordinate system

$$\frac{\partial u}{\partial x} + \frac{\partial v}{\partial y} = 0 \tag{1}$$

$$u \frac{\partial u}{\partial x} + v \frac{\partial u}{\partial y} = v_{nf} \frac{\partial^2 u}{\partial y^2} \tag{2}$$

$$u \frac{\partial T}{\partial x} + v \frac{\partial T}{\partial y} = \alpha_{nf} \frac{\partial^2 T}{\partial y^2} + \frac{(\rho c)_p}{(\rho c)_{nf}} \left[ D_B \frac{\partial \phi}{\partial y} \frac{\partial T}{\partial y} + \frac{D_T}{T_\infty} \left( \frac{\partial T}{\partial y} \right)^2 \right] \tag{3}$$

$$u \frac{\partial \phi}{\partial x} + v \frac{\partial \phi}{\partial y} = D_B \frac{\partial^2 \phi}{\partial y^2} + \left( \frac{D_T}{T_\infty} \right) \frac{\partial^2 T}{\partial y^2} \tag{4}$$

here,  $u$  and  $v$  are the velocity components along  $x$  and  $y$ -axis respectively,  $T$  is the temperature,  $\phi$  is the nanoparticle volume fraction,  $D_B$  is the Brownian diffusion coefficient,  $D_T$  is the thermophoretic diffusion coefficient,  $\rho$  is density,  $c$  is the specific heat capacity,  $\alpha = k/(\rho c)$  is the thermal diffusivity,  $\nu$  is the kinematic viscosity, and  $k$  is the thermal

conductivity. The subscripts  $nf$  and  $p$  refer to the nanofluid and nanoparticles, respectively. In this study, a Modified Single-Phase Model (MSPM) for analyzing nanofluids flow and heat transfer is introduced. For this manner, the parameters  $\nu_{nf}$ ,  $k_{nf}$ ,  $\rho_{nf}$ , and  $c_{nf}$  of the above governing equations can be replaced by the following relations [33]:

$$\begin{cases} \frac{(\rho c)_{nf}}{(\rho c)_f} = 1 - \phi + \phi \frac{(\rho c)_p}{(\rho c)_f} \\ v_{nf} = \frac{1}{(1 - \phi)^{2.5} (1 - \phi + \phi \rho_p / \rho_f)} \\ k_{nf} = \frac{k_p + 2k_f - 2\phi(k_f - k_p)}{k_p + 2k_f + \phi(k_f - k_p)} \end{cases} \tag{5}$$

where, the subscript  $f$  refers to the base fluid. The boundary conditions for the problem are given by:

$$\begin{aligned} u(x, 0) = u_w(x) = a_u x^n, v(x, 0) = v_w(x) = 0 \\ T(x, 0) = T_w(x) = a_T x^r + T_\infty, \phi(x, 0) = \phi_w \\ u(x, \infty) = 0, v(x, \infty) = 0, T(x, \infty) = T_\infty, \\ \phi(x, \infty) = \phi_\infty \end{aligned} \tag{6}$$

where,  $\phi_w$  and  $\phi_\infty$  are the nanoparticle volume fraction at the stretching surface and far away from the stretching sheet, respectively. By considering the following similarity transformations:

$$\begin{aligned} \eta = y\beta x^{\frac{n-1}{2}}, u = a_u x^n f'(\eta), \\ v = -\gamma x^{\frac{n-1}{2}} \left[ f + \frac{n-1}{n+1} \eta f' \right] \\ \theta(\eta) = (T - T_\infty) / (T_w - T_\infty), \\ \psi(\eta) = (\phi - \phi_\infty) / (\phi_w - \phi_\infty) \end{aligned} \tag{7}$$

(where,  $\beta = \sqrt{a_u(n+1)/(2\nu_f)}$  and  $\gamma = \sqrt{a_u \nu_f(n+1)/2}$ ) the BLF governing equations (1) to (4) are transformed to three ordinary differential equations as follows:

$$\begin{aligned} f''' + F(\phi) \left( f f'' - \frac{2n}{n+1} f'^2 \right) = 0 \\ \frac{1}{Pr(\phi)} \theta'' + f \theta' - \left( \frac{2r}{n+1} \right) f' \theta + \\ Nb(\phi) \psi' \theta' + Nt(\phi) \theta'^2 = 0 \\ \psi'' + \bar{Le} f \psi' + \frac{\bar{Nt}}{Nb} \theta'' = 0 \end{aligned} \tag{8}$$

where,

$$\begin{aligned} F(\phi) = (1 - \phi)^{2.5} (1 - \phi + \phi \rho_p / \rho_f) \\ Nb(\phi) = \bar{Nb} / \{1 - \phi + \phi (\rho c)_p / (\rho c)_f\} \\ Nt(\phi) = \bar{Nt} / \{1 - \phi + \phi (\rho c)_p / (\rho c)_f\} \\ Pr(\phi) = \nu_f / \alpha_{nf} = Pr_f \frac{k_p/k_f + 2 + 2\phi(1 - k_p/k_f)}{k_p/k_f + 2 - \phi(1 - k_p/k_f)} \\ \{1 - \phi + \phi (\rho c)_p / (\rho c)_f\} \end{aligned} \tag{9}$$

and,  $Pr_f = \nu_f/\alpha_f$  is the Prandtl number,  $\overline{Nb} = \{(\rho c)_p D_B(\varphi_w - \varphi_\infty)\}/\{\nu_f(\rho c)_f\}$  is the Brownian motion number,  $\overline{Nt} = \{(\rho c)_p D_T(T_w - T_\infty)\}/\{T_\infty \nu_f(\rho c)_f\}$  is the thermophoresis parameter, and  $\overline{Le} = \nu_f/D_B$  is the Lewis number. It is clear that,

$$\overline{Nb} = \{(\rho c)_p(\varphi_w - \varphi_\infty)\}/\{\overline{Le}(\rho c)_f\} \quad (10)$$

According to equations (6), equations (8) are solved subject to the following boundary conditions:

$$\begin{aligned} f'(0) = 1.0, \theta(0) = 1.0, \psi(0) = 1.0, f(\infty) = 0 \\ f'(\infty) = 0, \theta(\infty) = 0, \psi(\infty) = 0 \end{aligned} \quad (11)$$

By defining the local Reynolds number via  $Re_x = u_w(x)x/\nu_f = a_u x^{n+1}/\nu_f$ , the surface heat flux via  $q_w = k_{nf}(\partial T/\partial y)_{y=0}$ , the surface mass flux via  $q_m = D_B(\partial \varphi/\partial y)_{y=0}$ , the local Nusselt number via  $Nu_{nf} = xq_w/[k_{nf}(T_w - T_\infty)]$  and the local Sherwood number via  $Sh_{nf} = xq_m/[D_B(\varphi_w - \varphi_\infty)]$ , the following relation can be obtained:

$$\begin{cases} Nu_{nf} Re_x^{-1/2} = -\sqrt{(n+1)/2} \theta'(0) \\ Sh_{nf} Re_x^{-1/2} = -\sqrt{(n+1)/2} \psi'(0) \end{cases} \quad (12)$$

where,  $Nu_{nf} Re_x^{-1/2}$  and  $Sh_{nf} Re_x^{-1/2}$  are defined as dimensionless heat and mass transfer rates, respectively. Without loss of generality, one can assume that the nanoparticle volume fraction far away from the stretching sheet is zero or  $\varphi_\infty = 0$ . In this paper the fluid is a water based nanofluid containing different type of nanoparticles: copper (Cu), alumina ( $Al_2O_3$ ), titanium dioxide ( $TiO_2$ ). The thermophysical properties of the fluid and nanoparticles are given in Table 1 [33]. As the thermophysical properties of  $Al_2O_3$  and  $TiO_2$  are approximately the same, the simulation of Cu and  $Al_2O_3$  are only presented in result sections.

**Table 1**

Thermophysical properties of fluid and nanoparticles.

Properties	Fluid phase (water)	Cu	$Al_2O_3$	$TiO_2$
$c$ [J/kgK]	4179	385	765	686.2
$\rho$ [kg/m <sup>3</sup> ]	997.1	8933	3970	4250
$k$ [W/mK]	0.613	400	40	8.95
$\nu$ [m <sup>2</sup> /s]	$1.005 \times 10^{-6}$	-	-	-
$Pr_f$	6.83	-	-	-
$\rho_p/\rho_f$	-	8.959	3.981	4.262
$(\rho c)_p/(\rho c)_f$	-	0.825	0.729	0.700
$k_p/k_f$	-	652.53	65.25	14.60

## NUMERICAL ALGORITHM

The procedure of numerical calculation (computer program) of the non-linear differential equations(8-10)with

boundary conditions (11) is as follows:

- (i) Specify input data  $\rho_p/\rho_f$ ,  $(\rho c)_p/(\rho c)_f$ ,  $k_p/k_f$ ,  $Pr_f$ ,  $\overline{Nb}$ ,  $\overline{Nt}$ ,  $\overline{Le}$ , and  $\varphi_w$
- (ii) Set an initial guess for  $\varphi(\eta)$  or  $\psi(\eta)$
- (iii) Calculate  $F(\varphi)$ ,  $Nb(\varphi)$ ,  $Nt(\varphi)$ , and  $Pr(\varphi)$
- (iv) Solve the 1<sup>st</sup> relation of equation (8) to obtain  $f(\eta)$
- (v) Solve the 2<sup>nd</sup> relation of equation (8) to obtain  $\theta(\eta)$
- (vi) Solve the 3<sup>rd</sup> relation of equation (8) to update  $\psi(\eta)$  or  $\varphi(\eta)$
- (vii) Check the error between the updated  $\psi(\eta)$  and the guessed one.
- (viii) If the maximum error  $\leq 10^{-5}$  then the procedure is finished. If the maximum error  $> 10^{-5}$  the go to step (iii)

It should be noted that, for step (ii), by considering the assumption  $\varphi_\infty = 0$ , the initial guess can be  $\psi(\eta) = \varphi(\eta)/\varphi_w = (1 - e^{\eta - \eta_{max}})/(1 - e^{-\eta_{max}})$  as an example, where  $\eta_{max}$  is the maximum value of  $\eta$  in the numerical calculation.

## CODE VALIDATION

According to many references such as Ref. [25], [29], and etc., it is evident that the MSPM is reduced to the Prevalent Single-Phase Model (PSPM) by considering the relations:  $F(\varphi) = 1.0$ ,  $Nb(\varphi) = \overline{Nb}$ ,  $Nt(\varphi) = \overline{Nt}$ , and  $Pr(\varphi) = Pr$ . In order to check the validity of the present code (computer program), Equations (8-10) subject to the boundary conditions (11) are solved numerically for some values of the governing parameters of the prevalent single-phase model. The results for the reduced Nusselt number,  $-\theta'(0)$ , and the reduced Sherwood number,  $-\psi'(0)$ , are compared with those obtained by Khan and Pop [25] in Table 2.

**Table 2**

Comparison of results for  $-\theta'(0)$  and  $-\psi'(0)$  when  $Pr = 10$ ,  $\overline{Le} = 10$ ,  $n = 1$ ,  $r = 0$ , and  $\eta_{max} = 20$ .

Parameter	Present Result		Khan and Pop [25]	
	$-\theta'(0)$	$-\psi'(0)$	$-\theta'(0)$	$-\psi'(0)$
$\overline{Nb} = 0.1$ , $\overline{Nt} = 0.1$	0.95238	2.12939	0.9524	2.1294
$\overline{Nb} = 0.1$ , $\overline{Nt} = 0.3$	0.52007	2.52863	0.5201	2.5286
$\overline{Nb} = 0.1$ , $\overline{Nt} = 0.5$	0.32105	3.03514	0.3211	3.0351
$\overline{Nb} = 0.3$ , $\overline{Nt} = 0.1$	0.25215	2.41002	0.2522	2.4100
$\overline{Nb} = 0.3$ , $\overline{Nt} = 0.3$	0.13551	2.60882	0.1355	2.6088
$\overline{Nb} = 0.3$ , $\overline{Nt} = 0.5$	0.08329	2.75187	0.0833	2.7519
$\overline{Nb} = 0.5$ , $\overline{Nt} = 0.1$	0.05425	2.38357	0.0543	2.3836
$\overline{Nb} = 0.5$ , $\overline{Nt} = 0.3$	0.02913	2.49837	0.0291	2.4984
$\overline{Nb} = 0.5$ , $\overline{Nt} = 0.5$	0.01792	2.57310	0.0179	2.5731

In this simulation the default values of the parameters are considered as  $Pr = 10$ ,  $\overline{Le} = 10$ ,  $n = 1$ ,  $r = 0$ , and  $\eta_{max} = 20$ . It can be seen from Table 2 that the present results are in very good agreement with those reported by Khan and Pop [25]. Therefore, it is clear that the results obtained in this study are accurate.

**RESULTS AND DISCUSSION**

In order to get a clear understanding of the present problem, the numerical results for dimensionless velocity, temperature, nanoparticle concentration, and etc. are demonstrated in this section. Figures 2(a-f) and Figures 3(a-f) illustrate the effects of the two different nanoparticles (Cu and  $Al_2O_3$ ) on the dimensionless profiles for both MSPM and PSPM. The governing parameters for these simulations are given in Table 3.

In order to have a reasonable judgment between the results of PSPM and MSPM, the value of Brownian motion

number ( $\overline{Nb}$ ) for the PSPM is considered as the average of  $\overline{Nb}$  for Cu and  $Al_2O_3$ . The presented results in Figures 2 and 3 show that the temperature profiles converge quickly than the stream function profiles for both PSPM and MSPM. However, it is clear from the figures that the PSPM has a considerable deviation for predicting the behavior of nanofluids flow especially in dimensionless temperature ( $\theta$ ) and nanoparticle volume fraction ( $\psi$ ). From the results it is evident that, this inaccuracy is intensified when the sheet is stretched nonlinearly (see Fig. 3). Discussion about the PSPM and its effect on the results of the stretching sheet problem has been reported recently in many studies such as Refs. [25], [27], [29], and to name but a few. Therefore, the next simulations in this paper concentrate on the MSPM. As the boundary layer behavior and thermal characteristics of the both nanoparticles flow are approximately the same, the following results and discussion are focused only on Cu-water nanofluid flow and the MSPM.

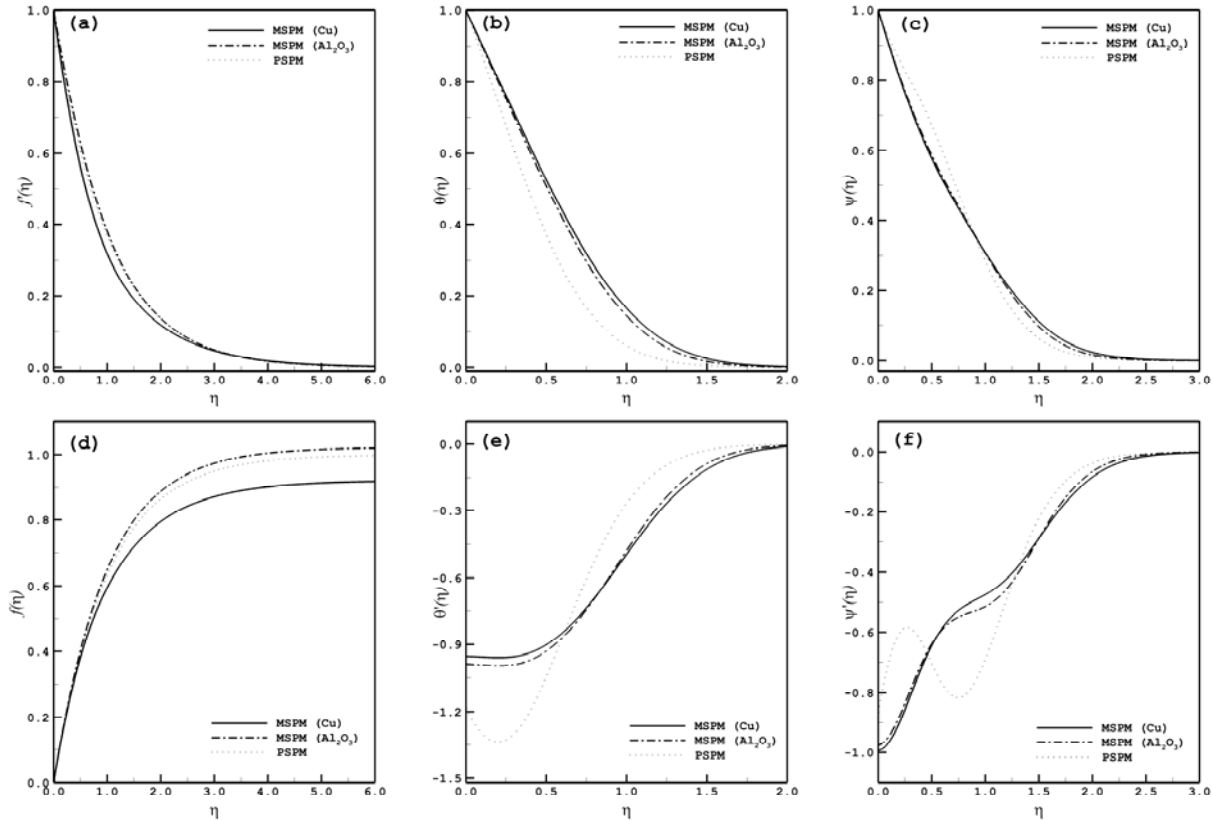


Fig. 2. Effect of the MSPM and PSPM on the dimensionless profiles ( $f, f', \theta, \theta', \psi, \psi'$ ) for Cu and  $Al_2O_3$ -water nanofluids,  $n = 1$ , and  $r = 0$

Plots of the dimensionless variables  $f'(\eta)$ ,  $\theta(\eta)$  and  $\psi(\eta)$  for Cu-water nanofluids with the governing parameters given in Table 3, are illustrated in Figures 4 through 7. Based on Figure (4a), the function  $f'(\eta)$  changes very little with  $\overline{Nt}$  changes.

However, Figures (4b) and (4c) show that as thermophoretic parameter ( $\overline{Nt}$ ) increases, the temperature and the volume fraction function (as well as the boundary

layer thickness for both items) increase for the specified conditions. This is because that, positive  $\overline{Nt}$  indicates a hot surface ( $T_w > T_\infty$ ).

For hot surfaces, thermophoresis tends to blow the nanoparticle volume fraction boundary layer away from the surface since a hot surface drives away the Nano-sized particles from it (increase in  $\psi$ ), thereby enhancing heat transfer process is occurred (increase in  $\theta$ ).

**Table 3**  
The governing parameters for nanofluid simulations.

Fig	Model	$n$	$r$	$\overline{Nt}$	$\overline{Le}$	$\phi_w$	$\overline{Nb}$	
2	MSPM (Cu)	1	0	0.1	5	0.5	0.0825	Eq. (10)
2	MSPM (Al <sub>2</sub> O <sub>3</sub> )	1	0	0.1	5	0.5	0.0729	Eq. (10)
2	PSPM	1	0	0.1	5	--	0.078	--
3	MSPM (Cu)	5	5	0.1	1	0.5	0.4125	Eq. (10)
3	MSPM (Al <sub>2</sub> O <sub>3</sub> )	5	5	0.1	1	0.5	0.3645	Eq. (10)
3	PSPM	5	5	0.1	1	--	0.3885	--
4, 7a	MSPM (Cu)	5	5	0.1~0.5	1	0.5	0.4125	Eq. (10)
5, 7b	MSPM (Cu)	5	5	0.1	1~50	0.5	0.4125~0.0082	Eq. (10)
6, 7c	MSPM (Cu)	5	5	0.1	1	0.3~0.5	0.2475~0.4125	Eq. (10)

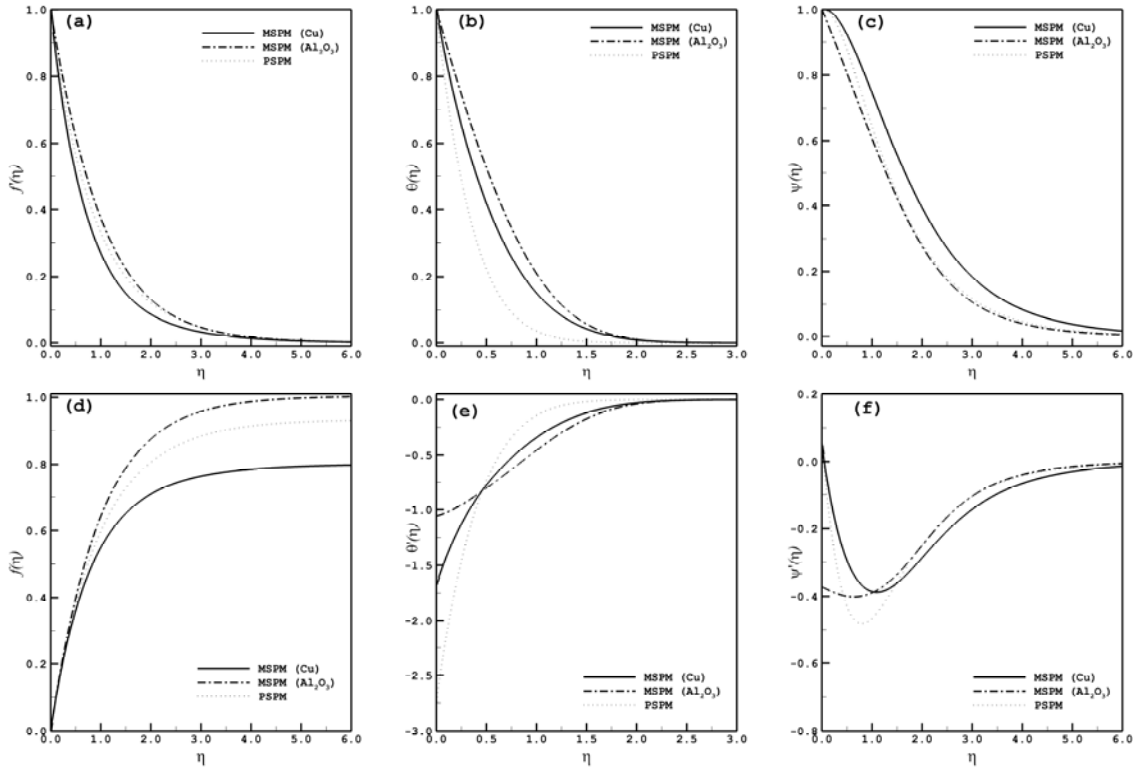


**Fig. 3.** Effect of the MSPM and PSPM on the dimensionless profiles ( $f, f', \theta, \theta', \psi, \psi'$ ) for Cu and Al<sub>2</sub>O<sub>3</sub>-water nanofluids,  $n = 5$ , and  $r = 5$

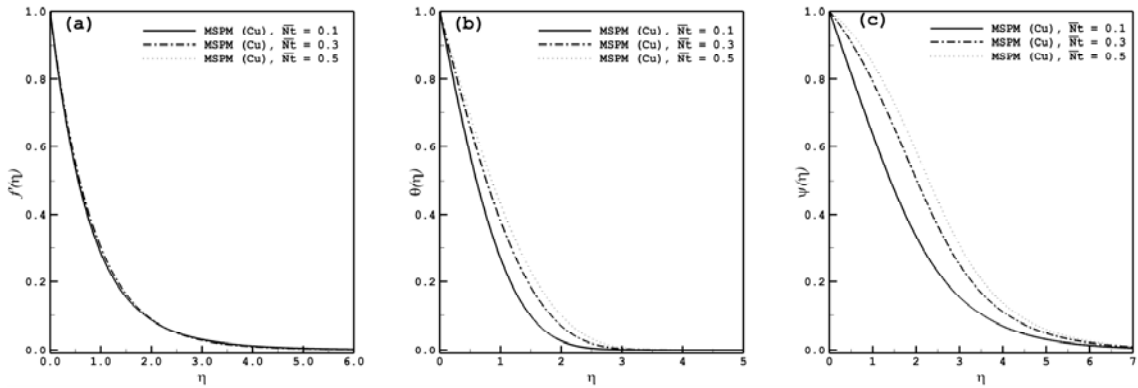


**Fig. 4.** Effect of  $\overline{Nt}$  on the dimensionless profiles ( $f, \theta, \psi$ ) for Cu-water nanofluids,  $n = 5$ , and  $r = 5$

Figure 5 demonstrates the effect of Lewis number ( $\overline{Le}$ ) on the velocity, temperature, and volume fraction distribution for selected values of  $\overline{Nt}$  and  $\varphi_w$ . One can see from Figure(5a) that  $\overline{Le}$  number has not a major effect on the velocity profile. However, it is remarked from Figs. 5b and 5c that the temperature and the volume fraction decrease with the increase in Lewis number. Lewis number is used to describe fluid flows where there is simultaneous heat and mass transfer and it presents the ratio of thermal diffusivity to mass diffusivity (Brownian diffusion coefficient,  $D_T$ ).

Therefore, the role of mass diffusion on heat transfer weakens with increasing Lewis number (or decreasing  $D_T$ ). Figure 6 represents the effect of the nanoparticle volume fraction at the stretching surface ( $\varphi_w$ ) on the velocity, temperature, and volume fraction distribution. It is evident from Figures (6b) that the temperature increases with the increase in  $\varphi_w$ . This behavior is because of the positive role of nanoparticle volume fraction near the surface on the heat transfer enhancement. In addition, according to Figures (6a) and (6c), it is clear that  $\varphi_w$  has a little influence on the velocity and volume fraction profiles.

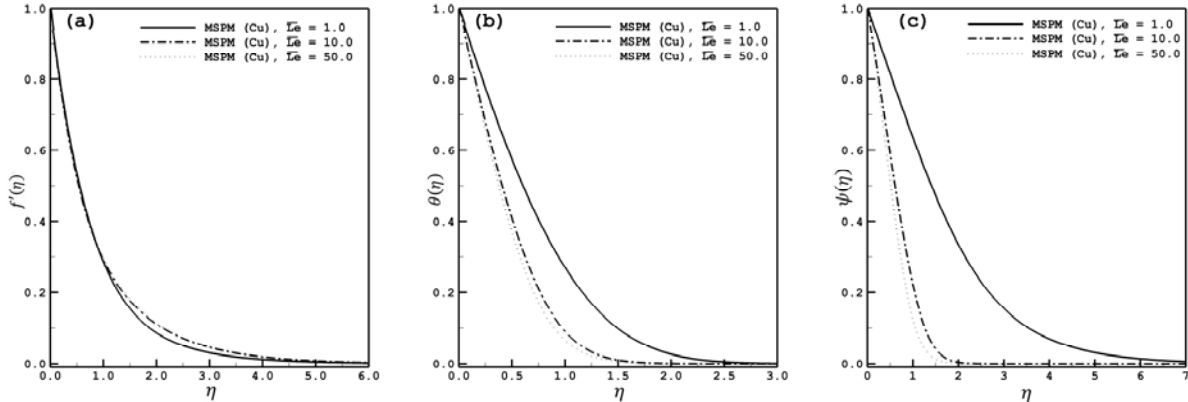


Fig. 5. Effect of  $\overline{Le}$  on the dimensionless profiles ( $f, \theta, \psi$ ) for Cu-water nanofluids,  $n = 5$ , and  $r = 5$

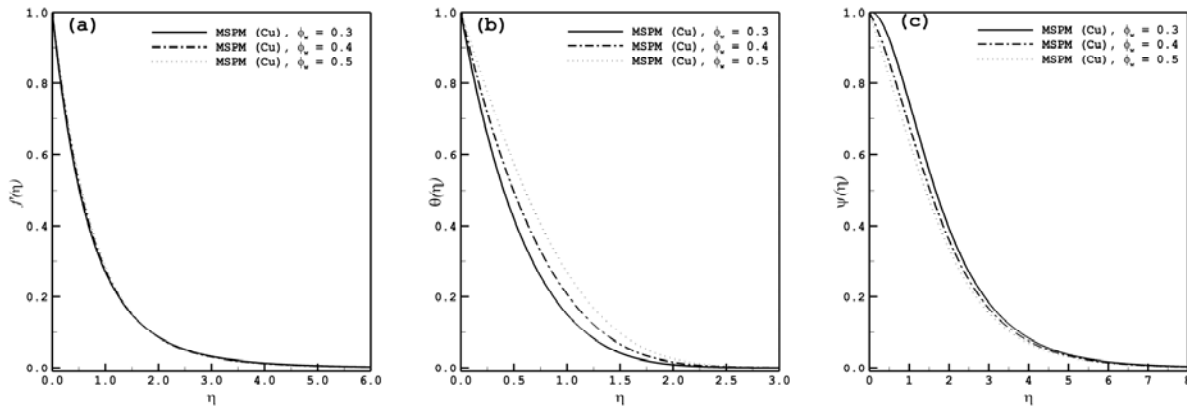


Fig.6. Effect of  $\varphi_w$  on the dimensionless profiles ( $f, \theta, \psi$ ) for Cu-water nanofluids,  $n = 5$ , and  $r = 5$ .

The last results are belong to the effect of  $\overline{Nt}$ ,  $\overline{Le}$ , and  $\varphi_w$  on the dimensionless heat and mass transfer rates. These results are plotted in Figure 7. Figure (7a) illustrates that heat and mass transfer rates decrease with the increase in  $\overline{Nt}$ . This is due to the fact that by increasing the thermophoresis parameter, the temperature and nanoparticles concentration increase near the solid surface as seen in Figures 4(b-c). However, based on Figure 7b,

heat and mass transfer rates increase with increase in  $\overline{Le}$ . The reason is that, when Lewis number increases, the temperature and nanoparticles concentration decrease near the solid surface as seen in Figures 6(b-c). Finally, a decrease in the dimensionless heat transfer and an increase in the dimensionless mass transfer are observed with increase in  $\varphi_w$ . This is shown in Figure (7c).

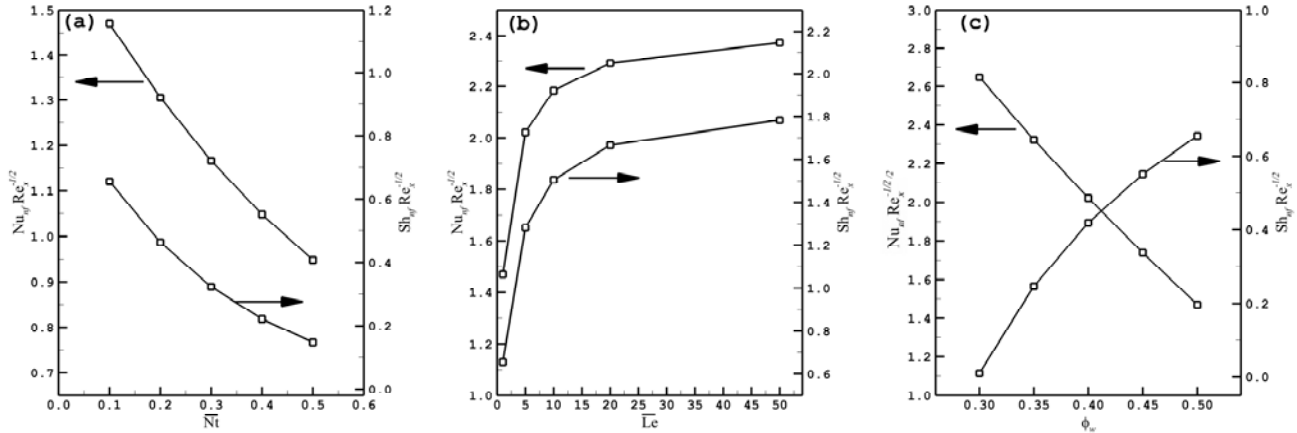


Fig.7. Effect of  $\overline{Nt}$ ,  $\overline{Le}$ , and  $\phi_w$  on the dimensionless heat and mass transfer rates for  $n = 5$  and  $r = 5$

## CONCLUSION

The benchmark problem of boundary layer nanofluid flow over a nonlinear stretching sheet is examined numerically. In this study, a modified variable physical properties model for analyzing nanofluids flow and heat transfer is initiated. In this modified model, the effective density and viscosity of nanofluids and the effective thermal conductivity of the solid-liquid mixture which are prevalently utilized in the effective single-phase model (as constant values), are incorporated locally with the governing equations (as no-constant values). A similarity solution is proposed which depends on the local Prandtl number, local Brownian motion number, local Lewis number, and local thermophoresis number. The results for Cu and  $Al_2O_3$  nanoparticles are compared to the prevalent single-phase model. This comparison shows that the prevalent single-phase model has a noticeable deviation for predicting the behavior of nanofluids flow especially in dimensionless temperature and nanoparticle volume fraction. In addition, the effect of the important governing parameters on the velocity, temperature, and volume fraction distribution and the heat and mass transfer rates are presented.

## ACKNOWLEDGEMENTS

The author would like to acknowledge the Shahrood University of Technology, which supported this project.

## REFERENCES

- [1] Hamad MA, Ferdows M. Similarity solutions to viscous flow and heat transfer of nanofluid over nonlinearly stretching sheet. *Applied Mathematics and Mechanics*. 2012 Jul 1;33(7):923-30.
- [2] Choi SU, Zhang ZG, Yu W, Lockwood FE, Grulke EA. Anomalous thermal conductivity enhancement in nanotube suspensions. *Applied physics letters*. 2001 Oct 1;79(14):2252-4.
- [3] Aminossadati SM, Ghasemi B. Natural convection cooling of a localised heat source at the bottom of a nanofluid-filled enclosure. *European Journal of Mechanics-B/Fluids*. 2009 Oct 31;28(5):630-40.
- [4] Xie H, Lee H, Youn W, Choi M. Nanofluids containing multiwalled carbon nanotubes and their enhanced thermal conductivities. *Journal of Applied physics*. 2003 Oct 15;94(8):4967-71.
- [5] Chol SU. Enhancing thermal conductivity of fluids with nanoparticles. *ASME-Publications-Fed*. 1995 Nov 12;231:99-106.
- [6] Abu-Nada E, Chamkha AJ. Mixed convection flow in a lid-driven inclined square enclosure filled with a nanofluid. *European Journal of Mechanics-B/Fluids*. 2010 Dec 31;29(6):472-82.
- [7] Sheikhzadeh GA, Arefmanesh A, Kheirkhah MH, Abdollahi R. Natural convection of Cu-water nanofluid in a cavity with partially active side walls. *European Journal of Mechanics-B/Fluids*. 2011 Apr 30;30(2):166-76.
- [8] Hassan H. Heat transfer of Cu-water nanofluid in an enclosure with a heat sink and discrete heat source. *European Journal of Mechanics-B/Fluids*. 2014 Jun 30;45:72-83.
- [9] Bourantas GC, Skouras ED, Loukopoulos VC, Burganos VN. Heat transfer and natural convection of nanofluids in porous media. *European Journal of Mechanics-B/Fluids*. 2014 Feb 28;43:45-56.

- [10] Rana P, Bhargava R. Flow and heat transfer of a nanofluid over a nonlinearly stretching sheet: a numerical study. *Communications in Nonlinear Science and Numerical Simulation*. 2012 Jan 31;17(1):212-26.
- [11] Yusoff NH, Uddin MJ, Ismail AI. Combined similarity-numerical solutions of MHD boundary layer slip flow of non-Newtonian power-law nanofluids over a radiating moving plate. *Sains Malaysiana*. 2014 Jan 1;43(1):151-9.
- [12] Abel S, Prasad KV, Mahaboob A. Buoyancy force and thermal radiation effects in MHD boundary layer visco-elastic fluid flow over continuously moving stretching surface. *International Journal of Thermal Sciences*. 2005 May 1;44(5):465-76.
- [13] Virto SL, Gamez-Montero PJ. Thin liquid film entrainment by moving solids. *Journal of Advanced Mechanical Design, Systems, and Manufacturing*. 2015;9(3):JAMDSM0024-.
- [14] Crane LJ. Flow past a stretching plate. *Kurze Mitteilungen - Brief Reports - Communications breves*. 1970; 21: 645-647.
- [15] Gupta PS, Gupta AS. Heat and mass transfer on a stretching sheet with suction or blowing. *The Canadian Journal of Chemical Engineering*. 1977 Dec 1;55(6):744-6.
- [16] Dutta BK, Roy P, Gupta AS. Temperature field in flow over a stretching sheet with uniform heat flux. *International Communications in Heat and Mass Transfer*. 1985 Jan 1;12(1):89-94.
- [17] Char MI. Heat transfer of a continuous, stretching surface with suction or blowing. *Journal of Mathematical Analysis and Applications*. 1988 Nov 1;135(2):568-80.
- [18] Vajravelu K. Viscous flow over a nonlinearly stretching sheet. *Applied mathematics and computation*. 2001 Dec 15;124(3):281-8.
- [19] Vajravelu K, Cannon JR. Fluid flow over a nonlinearly stretching sheet. *Applied Mathematics and Computation*. 2006 Oct 1;181(1):609-18.
- [20] Cortell R. Viscous flow and heat transfer over a nonlinearly stretching sheet. *Applied Mathematics and Computation*. 2007 Jan 15;184(2):864-73.
- [21] Prasad KV, Vajravelu K, Datti PS. Mixed convection heat transfer over a non-linear stretching surface with variable fluid properties. *International Journal of non-linear Mechanics*. 2010 Apr 30;45(3):320-30.
- [22] Postelnicu A, Pop I. Falkner-Skan boundary layer flow of a power-law fluid past a stretching wedge. *Applied Mathematics and Computation*. 2011 Jan 1;217(9):4359-68.
- [23] Vajravelu K, Prasad KV, Datti PS, Raju BT. MHD flow and heat transfer of an Ostwald-de Waele fluid over an unsteady stretching surface. *Ain Shams Engineering Journal*. 2014 Mar 31;5(1):157-67.
- [24] Bachok N, Ishak A, Pop I. Boundary-layer flow of nanofluids over a moving surface in a flowing fluid. *International Journal of Thermal Sciences*. 2010 Sep 30;49(9):1663-8.
- [25] Khan WA, Pop I. Boundary-layer flow of a nanofluid past a stretching sheet. *International journal of heat and mass transfer*. 2010 May 31;53(11):2477-83.
- [26] Van Gorder RA, Sweet E, Vajravelu K. Nano boundary layers over stretching surfaces. *Communications in Nonlinear Science and Numerical Simulation*. 2010 Jun 30;15(6):1494-500.
- [27] Hassani M, Tabar MM, Nemati H, Domairry G, Noori F. An analytical solution for boundary layer flow of a nanofluid past a stretching sheet. *International Journal of Thermal Sciences*. 2011 Nov 30;50(11):2256-63.
- [28] Nadeem S, Haq RU, Khan ZH. Heat transfer analysis of water-based nanofluid over an exponentially stretching sheet. *Alexandria Engineering Journal*. 2014 Mar 31;53(1):219-24.
- [29] Das K. Nanofluid flow over a non-linear permeable stretching sheet with partial slip. *Journal of the Egyptian Mathematical Society*. 2015 Jul 31;23(2):451-6.
- [30] Khanafer K, Vafai K, Lightstone M. Buoyancy-driven heat transfer enhancement in a two-dimensional enclosure utilizing nanofluids. *International journal of heat and mass transfer*. 2003 Sep 30;46(19):3639-53.
- [31] Buongiorno J. Convective transport in nanofluids. *Journal of Heat Transfer*. 2006 Mar 1;128(3):240-50.
- [32] Kuznetsov AV, Nield DA. Natural convective boundary-layer flow of a nanofluid past a vertical plate. *International Journal of Thermal Sciences*. 2010 Feb 28;49(2):243-7.
- [33] Oztop HF, Abu-Nada E. Numerical study of natural convection in partially heated rectangular enclosures filled with nanofluids. *International journal of heat and fluid flow*. 2008 Oct 31;29(5):1326-36.
- [34] Yazdi MH, Abdullah S, Hashim I, Sopian K. Slip MHD liquid flow and heat transfer over non-linear permeable stretching surface with chemical reaction. *International Journal of Heat and Mass Transfer*. 2011 Jul 31;54(15):3214-25.